Horizon 2020

| | |
|---|---|
| Project acronym: | **LASH FIRE** |
| Project full title: | **Legislative Assessment for Safety Hazard of Fire and Innovations in Ro-ro ship Environment** |
| Grant Agreement No: | **814975** |
| Coordinator: | **RISE Research Institutes of Sweden** |

LASH FIRE

# Internal Report IR09.15

# Evaluation of Detection Principles and Challenges in Early Detection of Thermal Runaway in Batteries

**September 2023**

Dissemination level: **Public**

## Abstract

The amount of battery electrical vehicles (BEVs) carried as cargo on ro-ro ships is increasing. The possibility of thermal runaway in a lithium-ion battery makes BEVs a different fire risk compared to internal combustion engine vehicles (ICEV). One of the challenges that arise is how to detect a thermal runaway early. Current detection systems in ro-ro spaces generally consist of smoke and/or heat detection. To identify potential techniques and challenges for detection of a thermal runaway, as early as possible, tests with batteries and detectors are needed.

Tests with one battery cell were performed inside an ISO container (with almost negligible ventilation) as well as in an open room with moderate ventilation (14 air changes per hour). Point-type detectors (two smoke and heat detectors, one CO detector, and one LEL detector), thermal imaging, video analytics, and light detection and ranging (LIDAR) were evaluated in the tests. A total of 14 tests were conducted. The detectors were evaluated in different positions relative to the battery cell and comparative tests with wood-sticks were performed to investigate the detectors' ability to detect a more conventional source of fire.

Based on the results, it can be concluded that early detection of thermal runaway in batteries is possible in principle. However, detection is a matter of circumstances e.g., ventilation, gas/smoke production and the location of the detector(s). The result indicates that detection in a small and confined space is relatively manageable, but detection in a large and open space could be more of a challenge. If the gas/smoke is cooled down it may sink and spread along the floor/deck, instead of rising and spreading along the ceiling. This would be a challenge with current smoke detectors installed in the ceiling. Shielding may be a problem, especially with LIDAR and thermal imaging. Future research should address full-scale tests, and it is recommended to include Optical Gas Imaging (OGI) as a mean of detection.

*This project has received funding from the European Union's Horizon 2020 research and innovation programme under grant agreement No 814975.*

*The information contained in this deliverable reflects only the view(s) of the author(s). The Agency (CINEA) is not responsible for any use that may be made of the information it contains.*

The information contained in this report is subject to change without notice and should not be construed as a commitment by any members of the LASH FIRE consortium. In the event of any software or algorithms being described in this report, the LASH FIRE consortium assumes no responsibility for the use or inability to use any of its software or algorithms. The information is provided without any warranty of any kind and the LASH FIRE consortium expressly disclaims all implied warranties, including but not limited to the implied warranties of merchantability and fitness for a particular use.

© COPYRIGHT 2019 The LASH FIRE Consortium

This document may not be copied, reproduced, or modified in whole or in part for any purpose without written permission from the LASH FIRE consortium. In addition, to such written permission to copy, acknowledgement of the authors of the document and all applicable portions of the copyright notice must be clearly referenced. All rights reserved.

# Document data

| | | | |
|---|---|---|---|
| Document Title: | IR09.15 – Evaluation of Detection Principles and Challenges in Early Detection of Thermal Runaway in Batteries | | |
| Work Package: | WP09 – Detection | | |
| Related Task(s): | T09.7, T09.8 | | |
| Dissemination level: | Public | | |
| Lead beneficiary: | 1 – RISE | | |
| Responsible author: | Sixten Dahlbom | | |
| Co-authors: | Martin Sanfridson, Ted Sjöblom | | |
| Date of delivery: | 2023-09-28 | | |
| References: | D09.2 | | |
| Approved by | Davood Zeinali on 2023-09-25 | Ola Willstrand on 2023-09-13 | Maria Hjolman on 2023-09-26 |

# Involved partners

| No. | Short name | Full name of Partner | Name and contact info of persons involved |
|---|---|---|---|
| 1 | RISE | Research Institutes of Sweden AB | Sixten Dahlbom – sixten.dahlbom@ri.se<br>Martin Sanfridson – martin.sanfridson@ri.se<br>Ted Sjöblom – ted.sjoblom@ri.se |
| | | | |
| | | | |
| | | | |
| | | | |

# Document history

| Version | Date | Prepared by | Description |
|---|---|---|---|
| 00 | 2023-07-07 | Sixten Dahlbom | Draft structure |
| 01 | 2023-09-11 | Sixten Dahlbom | Draft of final report, circulated to reviewers |
| 02 | 2023-09-27 | Sixten Dahlbom | Final report |
| | | | |
| | | | |

# Contents

# 1 Executive summary

## 1.1 Problem definition

The number of battery electrical vehicles (BEVs) transported as cargo on ro-ro ships is growing rapidly [1]. This is while the possibility of thermal runaway in a lithium-ion battery makes BEVs a different fire risk compared to internal combustion engine vehicles (ICEV). One of the challenges that arise is how to detect a thermal runaway early. Current detection systems in ro-ro spaces generally consist of smoke and/or heat detection. To identify potential techniques and challenges for detection of a thermal runaway, as early as possible, tests with batteries and detectors are needed.

## 1.2 Method

Tests with one battery cell were performed inside an ISO container (with almost negligible ventilation) as well as in an open room with moderate ventilation (14 air changes per hour). Four point-type detectors (two smoke and heat detectors, one CO detector and one LEL detector), thermal imaging, video analytics and light detection and ranging (LIDAR) were evaluated in the tests. A total of 14 tests were conducted. The detectors were evaluated in different positions relative to the battery cell and comparative tests with wood-sticks were performed to investigate the detectors' ability to detect a more conventional source of fire.

Previous internal reports within work package 09 (WP09) have provided input to this report, especially D09.2 [2] and IR09.14 [3]. There is no report dependent on the output from this report.

## 1.3 Results and achievements

All the evaluated point-type detectors were able to detect gas/smoke produced from the battery cell. The challenge with point-type detectors is to get the gas/smoke to the detector in concentrations high enough to be detectable. In a very small and confined space, this was not a problem. Inside a container, where the ventilation was negligible, detection was still possible. Tests in a room with moderate ventilation revealed that the point-type detectors failed to detect the gas/smoke.

When the smoke reached a steel surface and were cooled to the ambient temperature, the visible gases from the battery cell sank and spread along the floor (instead of rising and spreading along the ceiling). This could be a challenge in ship applications; conventional detectors are placed in the ceiling.

Thermal imaging worked very well, but only as long as the heat source/hot gases were visible from the camera's perspective. A handheld thermal imaging device could assist in manual firefighting.

Even though same type and SOC of the battery cells, an individual behaviour of the cells was observed. With most of the cells, a vigorous production of gas/smoke was observed. With some of the cells, the gas/smoke production was slower and lasted for longer times. As long as the gas/smoke production was not too low/slow, video analytics was able to the detect the smoke.

The LIDAR sensor was successful detecting smoke in its field-of-view, even the first venting event. A conclusion is that it should be feasible to implement a smoke detector for small and confined volumes.

## 1.4 Contribution to LASH FIRE objectives

This report addresses:

- Primary project objective: LASH FIRE will strengthen the independent fire protection of ro-ro ships by developing and validating effective operative and design solutions addressing current and future challenges[1] in all stages of a fire.
- Strategic objective: "To provide a recognized technical basis for the revision of international IMO regulations, which greatly enhances fire prevention and ensures independent management of fires on ro-ro ships in current and future fire safety challenges."
- The objective of WP09: Provide for quicker and more reliable fire detection, localization and confirmation in all types of ro-ro spaces by evaluation of new and advancing technologies.
- The goal of action (9-B): Develop, demonstrate and evaluate in full-scale alternative and complementing means for quick and reliable detection on closed and open ro-ro spaces.

## 1.5 Exploitation and implementation

The work was performed at the end of the LASH FIRE project. No deliverable depends on output/input from this work.

The gained knowledge will be shared externally through this report which will be publicly available on the LASH FIRE web site (www.lashfire.eu) and will lay a ground for future research in the area.

[1] The number of battery electrical vehicles is expected to increase further in the near future.

# 2 List of symbols and abbreviations

| | |
|---|---|
| ACH | Air Changes per Hour |
| BEV | Battery Electric Vehicle |
| BMS | Battery Management System |
| CO | Carbon Monoxide |
| ICEV | Internal Combustion Engine Vehicle |
| LEL | Lower Explosion Limit |
| LIDAR | Light Detection and Ranging |
| OGI | Optical gas imaging |
| VA | Video Analytics |
| WP | Work Package |

# 3 Terminology

The terminology in this report is in accordance with the LASH FIRE vocabulary and terminology used in the internal report "IR09 Early Detection of Thermal Runaway in Lithium-ion Batteries" [3]. A selection of the terms in the vocabulary is presented below.

**Battery electric vehicle (BEV):** Vehicle which is powered solely by battery electric energy.

**First venting:** The **first** vigorous ventilation from a Li-ion battery. First venting is (sometimes) proceeded by a small amount of a less vigorous gas release.

**Lithium-ion battery or Li-ion battery:** It is a type of rechargeable battery. Lithium-ion batteries are commonly used for portable electronics and electric vehicles. In these batteries, lithium ions move from the negative electrode to the positive electrode during discharge, and back when charging. Li-ion batteries use an intercalated lithium compound at the material on the positive electrode and typically graphite at the negative. There are however many different active materials available for use at the positive and negative electrodes which result in a large family of different types of Li-ion batteries with different characteristics. Compared to other types of batteries, Li-ion batteries have a high energy density, no memory effect and low self-discharge.

**Propagation:** When the heat produced in one of the battery cells is sufficient to heat an adjacent battery cell and trigger thermal runaway also in this cell. The propagation continues from cell to cell and often leads to a cascading scenario in surrounding battery cells.

**Thermal runaway:** A scenario where the stored chemical energy of a battery cell, by internal exothermic reactions, is converted to thermal energy.

# 4 Introduction

Main author of the chapter: Sixten Dahlbom, RISE

The number of battery electric vehicles (BEVs) transported by ships is increasing [1]. Li-ion batteries pose a certain fire risk due to their organic electrolyte and the nature of thermal runaway and poor accessibility in case of a fire. Further, there is also a risk of thermal runaway and propagation, resulting in a rapid fire growth. Thermal runaway refers to an event when one battery cell heats up in an uncontrolled manner. Typically, this results in pressure relief through the ventilation of gases from the cell to the surrounding. The gases may, or may not, ignite (depending on ignition sources and state of charge (SOC)). Propagation refers to the event when heat spreads from one battery cell to other(s), resulting in thermal runaway in this/these cell(s) as well.

Typical fire detectors used in ro-ro spaces are point-type heat and/or smoke detectors. The aim of this study was to perform tests in a small- to intermediate-scale to evaluate if the currently used, or other, detectors can detect a thermal runaway of a battery cell in an early stage. In this case, an early stage refers to ventilation of gases from one battery cell. In the current study, the gases were not supposed to ignite since this was considered to no longer fall under the scope of “early detection of thermal runaway”.

The aim of this study was to identify techniques of potential interest for further evaluation. The aim was also to identify challenges with early detection of thermal runaway in a battery cell. The scope was not to perform tests fully generalisable to all battery thermal runaway events.

To evaluate different detection techniques’ ability to detect initial/early stages of a thermal runaway in a battery cell, tests were conducted at RISE’s facility in Borås in July 2023. The evaluated detection techniques were selected partially based on annex B of report D09.2 [2] and partially after approaching different manufacturers and asking for their interest to participate.

# 5 Method

Main author of the chapter: Sixten Dahlbom, RISE

This chapter contains a description of the detectors and the test setup. Four point-type detectors and three camera-based technologies were evaluated in the test series. A total of 14 tests were performed, ten of them with a single battery cell and four of them with wood-sticks on a hot plate.

## 5.1 Detectors

The detectors were selected based on the internal report D09.2 – Developed ro-ro spaces fire detection solutions and recommendations [2], but also on interest and availability of detection manufacturers/suppliers and their equipment.

Five of the detectors were coupled with an alarm system i.e., there was a logic that triggered an alarm if certain requirements were fulfilled (cf. Table 1 for alarm conditions). With these detectors, there is a risk that the alarm conditions (which serve as filters to avoid false alarms) will exclude short-lived events.

Two of the camera-based detectors did only produce a video recording, which had to be manually postprocessed and interpreted. These two detectors were included to evaluate if they are suitable for detection and whether there is a possibility to complement these two camera-based detectors with an alarm algorithm in the future.

The detectors included in the study were: two types of combined smoke and heat detectors; a carbon monoxide (CO) detector; a lower explosion limit (LEL) detector; video analytics (VA); thermal imaging; and light detection and ranging (LIDAR).

### 5.1.1 Point-type detectors

Point-type detectors are fixed detectors with detection in a single point. This means that the point of the detection must be in contact with gas, smoke, or heat to enable detection. The point-type detectors all produced alarms in case of detection. The point-type detectors were the combined smoke and heat detectors, the CO detector, and the LEL detector.

### 5.1.2 Camera-based detectors

Three camera-based detectors were included in the study. Being camera-based means that one detector sees everything in the region that is visible to the camera lens.

Video Analytics (VA) is based on a regular surveillance camera and a computer algorithm that interprets the image to identify smoke or flames (other functions are available but were not included in the current study). Thermal imaging detects any source of heat, and it produces an image of the room. LIDAR uses light of a defined wavelength to map the room, while smoke will interfere with the light, so it could be detected. Benefits of thermal imaging and LIDAR is that they are not sensitive to light conditions in a room. Thermal imaging and LIDAR were not coupled with an alarm system.

### 5.1.3 Alarm conditions

The principles of when an alarm was triggered or when a thermal runaway event was detected by the detectors are presented in Table 1.

*Table 1. Summary of the detectors and alarm conditions.*

<table>
<tr><th>Detection principle</th><th>Alarm condition(s)</th></tr>
<tr><td>Combined smoke and heat detector 1</td><td>• Smoke: 0.19 dB/m<br>• Heat: 54 °C or heat rise according to:
<table>
<tr><th>Rate of temperature rise [°C/min]</th><th>Lower limit of response time [min:s]</th><th>Upper limit of response time [min:s]</th></tr>
<tr><td>1</td><td>29:00</td><td>40:20</td></tr>
<tr><td>3</td><td>07:13</td><td>13:40</td></tr>
<tr><td>5</td><td>04:09</td><td>08:20</td></tr>
<tr><td>10</td><td>01:00</td><td>04:20</td></tr>
<tr><td>20</td><td>00:30</td><td>02:20</td></tr>
<tr><td>30</td><td>00:20</td><td>01:40</td></tr>
</table></td></tr>
<tr><td>Combined smoke and heat detector 2</td><td>• Smoke: 0.12 dB/m<br>• Heat: 54 °C or heat rise according to:
<table>
<tr><th>Rate of temperature rise [°C/min]</th><th>Lower limit of response time [min:s]</th><th>Upper limit of response time [min:s]</th></tr>
<tr><td>1</td><td>29:00</td><td>40:20</td></tr>
<tr><td>3</td><td>07:13</td><td>13:40</td></tr>
<tr><td>5</td><td>04:09</td><td>08:20</td></tr>
<tr><td>10</td><td>01:00</td><td>04:20</td></tr>
<tr><td>20</td><td>00:30</td><td>02:20</td></tr>
<tr><td>30</td><td>00:20</td><td>01:40</td></tr>
</table></td></tr>
<tr><td>CO detector</td><td>• First alarm at 50 ppm CO<br>• Second alarm at 70 ppm CO</td></tr>
<tr><td>LEL detector</td><td>• First alarm at 10 % of LEL<br>• Second alarm at 15 % of LEL</td></tr>
<tr><td>Video analytics</td><td>• Alarm was only allowed to be triggered if smoke or flame(s) was detected within a pre-defined zone. This was done to avoid false alarms.<br>• The sensitivity was set to “medium” (according to the supplier’s instructions)<br>• A 5 s delay was applied.</td></tr>
<tr><td>Thermal imaging</td><td>• Measurement data logged during the tests and manually post-processed.</td></tr>
<tr><td>LIDAR</td><td>• Measurement data logged during the tests and manually post-processed.</td></tr>
</table>

### 5.1.4 Video Analytics

Supplier: FIKE

*According to the supplier:*

A prolific context has become available for new applications of video fire detection in shipboard safety systems due to significant progresses made in computer processing, video imaging cameras, and video analytics for the detection of oil mist, smoke, flame, and flame reflections. In the maritime environment, video analytics is widely used in cruise ship machinery spaces monitoring for early signs of oil mist in the atmosphere.

Existing video surveillance infrastructure and off-the-shelf IP CCTV cameras are utilized, providing an economical, reliable, and proven early detection solution with server-based analytics. Video analytics servers include the latest high-speed computer processors, commonly used Windows operating systems and proprietary video analytics software based on artificial intelligence-derived algorithms.

Video analytics detects smoke by monitoring the light level in all the pixels of the field of view. When smoke moves through the image, the light level changes in the group of pixels, and the affected

pixels show a rise in elevation and spread out into a plume. The video analytics algorithms that were trained using machine vision recognize this and track the smoke until the sensitivity parameters are met, at which time the system produces an alarm.

The crew can easily locate the event area, coordinate the fire-fighting response, or activate and monitor a fire suppression system based on live video information.

Classification societies see the benefit of this technology as included in the recently published DNVGL-RU-SHIP Pt.6 Ch.5 Equipment and Design Features [4] that recommends video analytics as a solution in machinery spaces for “rapid oil mist detection”.

### 5.1.5 Combined smoke and heat detector 1

Supplier: Consilium

Model: CD-PH

The sensors were optical light scattering and thermistor, class A1R. According to the supplier, there is a difference in the construction, compared to the combined smoke and heat detector 2.

### 5.1.6 Combined smoke and heat detector 2

Supplier: Consilium

Model: CD-PH EX ic

The sensors were optical light scattering and thermistor, class A1R. According to the supplier, there is a difference in the construction, compared to the combined smoke and heat detector 1.

### 5.1.7 CO-detector

Supplier: Consilium

Model: Gas detector ST450 EC configured for CO detection

*According to the supplier’s datasheet:*

The detector is an all-round gas detector which functions well under most circumstances. The measuring principle is based on an electrochemical sensor. The sensor has a good stability, which achieves long-term reliability. The high selectivity of the sensor minimalizes “false” readings. The sensor is Ex d and Ex t approved (ATEX and IECEx).

### 5.1.8 LEL-detector

Supplier/Manufacturer: Consilium

Model: Gas Detector ST 650 EX

*According to the supplier’s datasheet:*

The ST 650 EX is an all-round gas detector which functions well under the most difficult circumstances. The detector was configured with a molecular property spectrometer (MPS) sensor. The sensor can differentiate 14 different flammable gases.

### 5.1.9 Thermal Imaging

Supplier/Manufacturer: FLIR
Model: A500

*According to the supplier:*

FLIR A500 thermal cameras offer researchers and engineers a streamlined solution for accurate temperature measurements. Simplified yet robust connections help you set up and start testing quickly; then easily view, acquire, and analyse data using included FLIR Research Studio software. The A500 (464 × 348 pixels, spectral range 7.5–14.0 µm, temperature range -20 °C to 1 500 °C) image streaming camera has a 24° lens with automatic/remote and manual focusing, as well as FLIR Macro Mode.

### 5.1.10 LIDAR

Supplier/Manufacturer: Ouster

Model: OS2, 128 layers, hardware revision D

The lidar sensor measures the time it takes for the emitted laser pulse to travel to the object and back to the sensor. This is done using a detector that can measure the time delay with high precision. This lidar has been developed primarily for the vehicle industry to map the geometry of its environment. The output is a point cloud with information of geometry, intensity in reflection, and in the case of an Ouster 2 lidar, an image of background IR radiation. A detection of the fire will be based on tracking changes, primarily the damping of returned intensity. There is also a possibility to pick up aerosols depending on their size and distance from the sensors.

## 5.2 Test setup

To challenge the detectors and to gather as much input as possible, tests with different setups were considered, namely, tests were conducted both in a large hall with approximately 14 air changes per hour (ACH) and inside a 20-ft ISO container [5] with nearly no ventilation. In some of the tests, the battery cell was covered by a hood (a metallic hexahedron with one side open, cf. Figure 3). This was done to evaluate a case where the battery cell is covered. All tests were performed indoors, where the temperature was typically between 20 °C and 25 °C.

Seven types of test setups were evaluated through a total of 14 tests. Ten of the tests addressed early detection of thermal runaway in battery cells, while four of the tests were performed with wood-sticks on a hot plate. The test procedure with wood-sticks was inspired by EN 54-7 [6] (e.g., by placing the detectors on an arc on the ceiling, using wood-sticks, using a hot plate to ignite wood-sticks, the use of a relatively confined space), but with adaptions according to the needs of the current study (cf. section 5.2.4). Tests with wood-sticks were conducted to get an idea of how the detectors perform in the case of a more conventional/classical fire scenario. A summary of the conducted tests is given in Table 2 and in the following sections.

*Table 2. Summary of the 14 tests conducted.*

| Test | Short description |
|---|---|
| 1, 2 | Free-standing battery cell in a ventilated room with 14 ACH. |
| 3 | Battery cell covered by a hood and further shielding in front of the thermal imaging camera, test in a ventilated room with 14 ACH. |
| 4 | Battery cell covered by a hood, in a ventilated room with 14 ACH. |
| 5, 6 | Wood-sticks on a hot plate, in a ventilated room with 14 ACH. |
| 7, 8, 9 | Free-standing battery cell inside a 20-ft container. |
| 10, 11 | Wood-sticks on a hot plate, inside a 20-ft container. |

| | |
|---|---|
| 12, 13 | Battery cell covered by a hood, inside a 20-ft container, the point-type detectors placed in the ceiling. |
| 14 | Battery cell covered by a hood, inside a 20-ft container, the point-type detectors placed in the hood. |

Thermal runaway was triggered by slowly heating the battery cell with flexible polyimide heaters with an adhesive backing. One heater (180 W) was attached to the battery cell. The temperature on the surface of the battery cell under the heater was continuously measured and used to control the heating. The temperature ranged were selected to be slow, to avoid ignition of the gases. The selection of the ramps was made based on internal, unpublished, knowledge. Following temperature ramps were used in the tests (the ramp was changed to shorten the time for the tests, it was however deemed to not impact the result):

- Test 1 – Test 2: 3 °C/min up to 65 °C, 1 °C/min thereafter
- Test 3 – Test 12: 3 °C/min up to 65 °C, 2 °C/min up to 165 °C, 1 °C/min thereafter
- Test 13 – Test 14: 3 °C/min up to 110 °C, 2 °C/min up to 165 °C, 1 °C/min thereafter

All the battery cells were of the same type. They were prismatic cells manufactured by ETC battery and had a capacity of 53 Ah (at 25 °C). A photo of one of the cells is presented in Figure 1. SOC varied between 49 % and 50 % (3.6 V) in all the tests. The SOC was selected to be low enough to avoid ignition of the gas released during ventilation, but also to be representative of a general BEV. It was decided to use a single battery cell since the focus of this study was detection of *early* thermal runaway, and thermal runaway likely starts in one cell (and then possibly propagates to adjacent cells).

*Figure 1. Photo of one of the battery cells used in the tests.*

### 5.2.1 Test 1 & 2 – Free-standing battery cell in a ventilated room

In these tests, the battery cell was free-standing. The vent opening/burst disc on the battery cell was directed upwards, to the ambient. A photo of the setup is shown in Figure 2. The figure also contains indications of where the detectors were installed and what measurements were made by the different detectors. The point-type detectors i.e., the two smoke and heat, the CO, and the LEL detectors were installed approximately 1.8 m above the battery cell. The other detectors (LIDAR, VA, and thermal imaging) were installed further away from the cell (cf. Figure 2).

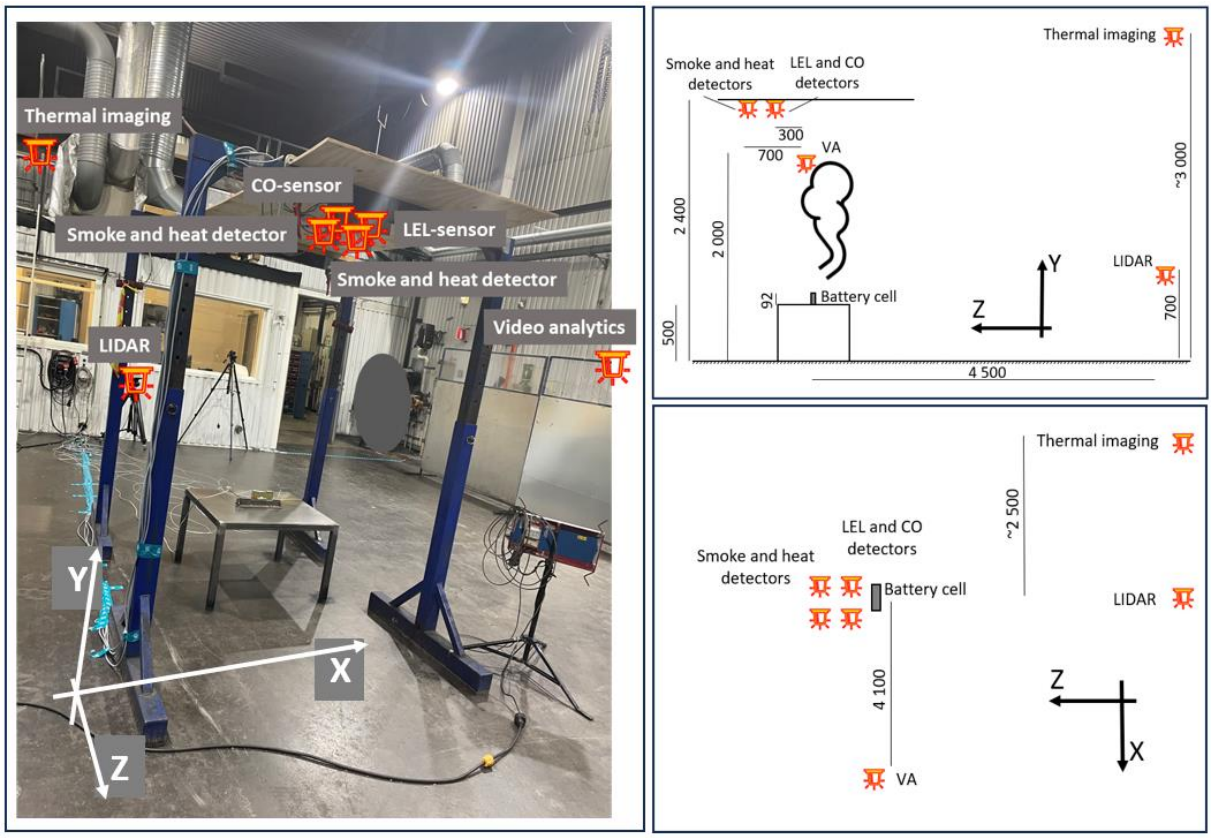


*Figure 2. Left: Photo of the test setup. The locations of the different detectors are indicated in the photo. Right: Locations of the detectors relative to the battery cell (measures in mm).*

A free-standing battery cell was considered to be the easiest case for early detection of thermal runaway. Given that the point-type detectors must be in contact with the smoke, it was decided to install them above the battery. Because of the risk of a jet flame from the battery (if released gases ignited), the detectors were installed slightly off-centred from just above of the battery cell. The thermal imaging camera, the video analytics camera and the LIDAR sensor were placed further away from the battery cell, as per the suppliers' instructions.

### 5.2.2 Test 3 – Battery cell covered by a hood and further shielding, in a ventilated room

In this test, the battery cell was covered by a hood compartment (cf. Figure 3). The hood (0.7 m × 0.7 m × 0.3 mm) was made of steel and had 25 mm of rockwool insulation on its outside, with only one small opening (50 mm x 50 mm). To further challenge the thermal imaging technology, the hood and battery cell were shielded by a steel plate placed between the thermal imaging camera's lens and the battery cell (which was covered by the hood) i.e., the thermal imaging camera was not able to directly see the battery cell nor the covering hood (cf. Figure 3, right).

The detectors for thermal imaging, video analytics and LIDAR were kept at the same positions as in the first two tests (cf. Figure 2). The CO and the LEL detectors were moved and placed inside the hood[2], just next to the battery cell (cf. Figure 3, left). The two smoke and heat detectors were not in use in this test.

[2] One question was if the CO and LEL detectors were able to detect the gases from a thermal runaway event, if installed in an enclosed space (e.g., inside the battery casing). Therefore, these two detectors were installed inside the hood.


*Figure 3. Left: Photo of the hood with the CO and LEL sensors. The 50 mm × 50 mm opening was there to allow a controlled release of gases. Right: The hood and the shielding covering the battery cell.*

The aim of this test was to capture the behaviour of a covered battery cell, as is the case when a cell is inside e.g., a battery casing or car chassis. To cover the battery cell, the hood mentioned above was used. A battery cell is, in reality, likely to be covered/shielded by the battery casing, the BEV itself, other cars, cargo, etc.

### 5.2.3 Test 4 – Battery cell covered by a hood, in a ventilated room

This test was almost identical to Test 3. The only difference was that the "further shielding" i.e., the uppermost steel plate, was removed. This was done after it was observed that the thermal imaging device was not able to detect any temperature change in Test 3.

### 5.2.4 Test 5 & 6 – Wood-sticks on a hot plate, in a ventilated room

The test setup was identical to the setup in Test 1 and Test 2. However, the battery cell was replaced with eight pieces (75 mm × 45 mm × 20 mm) of pine placed on a hot plate (cf. Figure 4). The aim was to evaluate the detectors additionally with a more conventional fire source, providing a basis of comparison against the tests performed with battery cells.

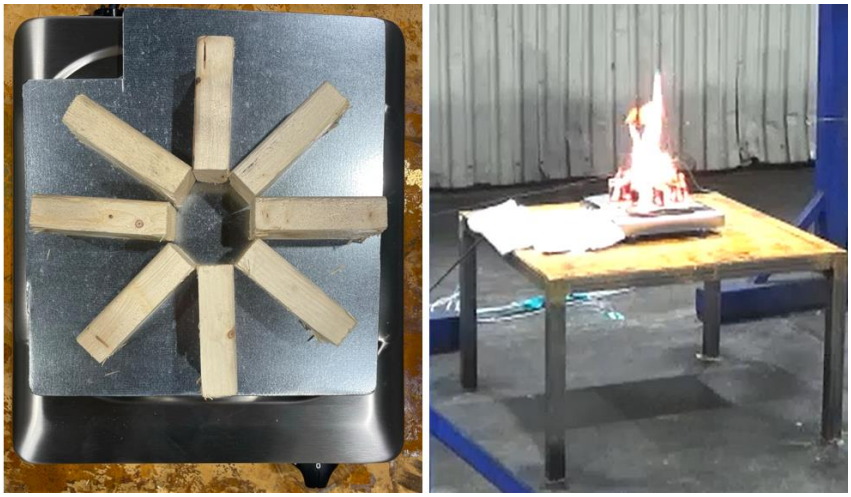

*Figure 4. Left: Wood-sticks on the hot plate. Right: Burning wood-sticks.*

### 5.2.5 Test 7, 8 & 9 – Free-standing battery cell inside a 20-ft ISO container

Test 7, Test 8, and Test 9 were similar to Test 1 and Test 2. A free-standing battery cell (not covered) was placed with the burst disc directed upwards. Photos of the setup are shown in Figure 5. The figure also contains indications of where the detectors were installed. Figure 6 contains an

illustration of the different detectors' locations. One of the doors on the container was kept closed during the tests. The other door was kept open to allow for the thermal imaging camera, the LIDAR, and the video analytics camera to be placed outside the container. The reason for conducting the tests in an ISO container was to keep air turbulence to a minimum and reduce variations in the tests.


*Figure 5. Top left: The container and some of the detectors (outside of the container). Top right: The inside of the container and the location of the detectors. Bottom left: A photo of some of the data acquisitioning systems. Bottom right: A free-standing battery cell and detectors on the ceiling inside the container.*

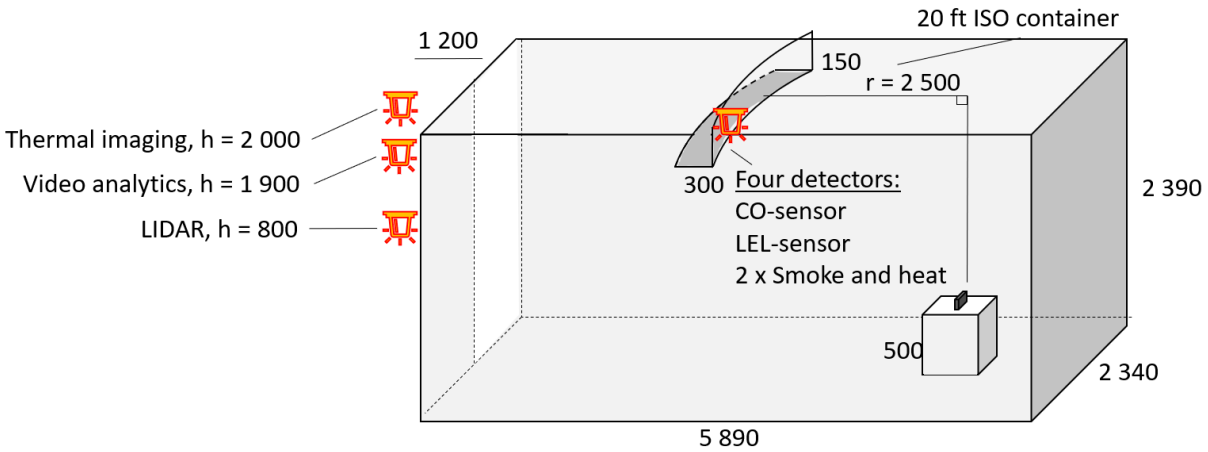


*Figure 6. Locations of the detectors relative to the battery cell (measures in mm).*

### 5.2.6 Test 10 & 11 – Wood-sticks on a hot plate, inside a 20-ft ISO container

The test setup was identical to the setup in Test 7, Test 8, and Test 9. However, the battery cell was replaced with eight pieces (75 mm × 45 mm × 20 mm) of pine placed on a hot plate (cf. Figure 4).

### 5.2.7 Test 12 & 13 – Battery cell covered by a hood, inside a 20-ft ISO container

In this test, the battery cell was covered by the same hood as that used in Test 3 and Test 4 (cf. Figure 3). All the detectors (thermal imaging, video analytics, LIDAR, CO and the smoke and heat detectors) were kept at the same positions as those in Test 10 and Test 11 (cf. Figure 5 and Figure 6).

### 5.2.8 Test 14 – Battery cell covered by a hood, inside a 20-ft ISO container

In this final test, which was similar to Test 12 and Test 13, the CO and the two smoke and heat detectors were installed inside the hood covering the battery cell.

# 6 Result

Main author of the chapter: Sixten Dahlbom, RISE

Of the 14 tests conducted, 10 were performed with the 53 Ah battery cells (49–50 % SOC) and four with wood sticks on a hot plate. behaviours of the battery cells were similar, although not identical. The first thing that was typically observed was a release of a very small, barely visible, amount of smoke. This was followed by an event with extensive smoke production lasting for a couple of seconds (this more vigorous event is in this work referred to as “first venting”). A photo and a snapshot from the thermal imaging of first venting is shown in Figure 7. The first venting was most often followed by a period with less (or no) smoke production. That period lasted for approximately 10–15 min. After that, the temperature of the battery cell increased rapidly (thermal runaway), and more smoke was produced. For three of the battery cells, the first venting was relatively mild, and no thermal runaway was observed. Instead, the gas/smoke production was less vigorous and lasted much longer compared to the other 11 tests.

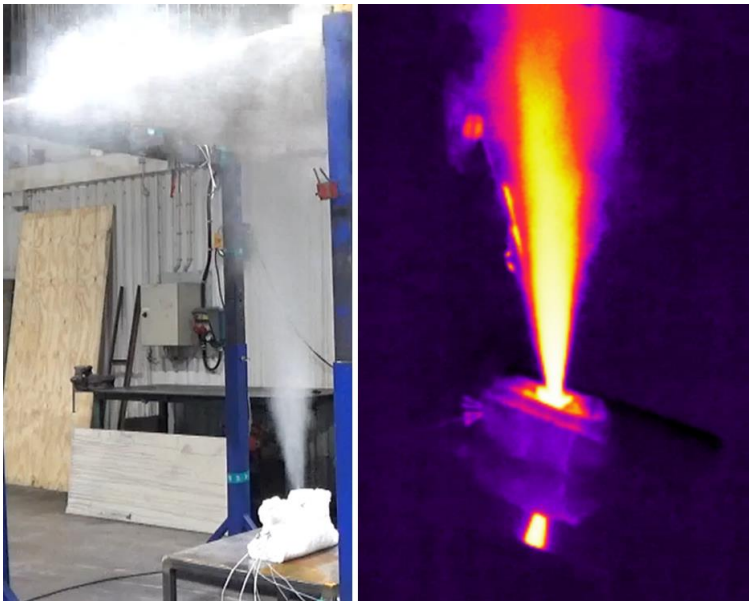

*Figure 7. Left: Photo of ventilation during first venting. Right: Snapshot from thermal imaging during first venting.*

Table 3, Table 4, Table 6, Table 8 and Table 9 contain times to detection from the tests with battery cells. The time to detection is counted from first venting. First venting was used as reference because the event was easy identifiable, both visually and by temperature readings. For an unknown reason, the LEL detector stopped working after Test 4 and is therefore not included in all tables.

With regard to the CO and LEL detectors, the result tables contain manual readings from the centrals. Therefore, different concentrations are sometimes presented.

## 6.1 Detectors with an alarm algorithm

### 6.1.1 Tests 1 and 2

The results of Test 1 and Test 2 are presented in Table 3. In these tests, the gas/smoke did not reach the point-type detectors (i.e., the smoke and heat, CO, and LEL detectors) in concentrations high enough to trigger any alarm was triggered. In Test 1, the point-type detectors were fully covered by visible smoke (cf. Figure 8, left), but an alarm was not triggered. In Test 2, the release of gas/smoke was milder/slower (cf. Figure 8, right). In Test 1 and Test 2, smoke was produced, but VA was the only detector able to detect the smoke. Even though the point type detectors were covered by

smoke visible to the eye, it was for some reason not enough to trigger detection by the point-type detectors.

*Table 3. Summary of detection results (min:s) from tests with a battery cell in a relatively open and ventilated space. F = Flame. S = Smoke. Det. = Detection*

| Test | First visible smoke | Video analytics | Smoke and heat detector 1 | Smoke and heat detector 2 | CO detector | LEL detector |
|---|---|---|---|---|---|---|
| 1 | -03:41 | 08:39 (F) | No det. | No det. | No det. | No det. |
| 2 | -01:52 | 13:58 (F)<br>14:03 (S) | No det. | No det. | No det. | No det. |

*Figure 8. Right: Smoke covering the point-type detectors in Test 1. Left: The less vigorous production of gas/smoke in Test 2.*

In both tests, VA registered flames, even though there were no flames, only smoke. In Test 1, when the smoke production was more intense, the time to (flame) detection by VA, was more than five minutes shorter than in the time in Test 2. In Test 2, smoke was identified by VA shortly after VA had detected flames.

The results indicate a potential challenge with point-type detectors in an open space for early detection of gas/smoke released from thermal runaway in batteries. In this study, the detectors were installed almost just above the battery cell, which will likely not be the case in e.g., a ro-ro space (there will likely be a big difference in heights). VA struggled initially with false alarms caused by changing light conditions in the test hall, to deal with this, the windows had to be covered before the tests (which solved the problem). VA detected the thermal runaway event 8–14 min after first venting.

### 6.1.2 Tests 3 and 4

The results of Test 3 and Test 4 are presented in Table 4. Since the cell was covered by a hood during these tests[3], the small amount of smoke produced before the event of first venting was not possible to confirm visually.

[3] In Test 3, the hood itself was further shielded by a steel plate as explained in section 5.2.3, but this only affected thermal imaging, while the results for the other detectors should otherwise be comparable for Test 3 and Test 4.

The gas released from the cell leaked out from the hood to the ambient from the bottom of the hood. Instead of rising (as was observed in Test 1 and Test 2), the *visible* gas/smoke sank and spread along the floor (cf. Figure 9, left). It is expected that this was due to the cooling of the gas by the hood (which was estimated to weigh approximately 15 kg). Cooling of the gas was further supported by thermal imaging. Such cooling could increase the density of the gas to beyond that of the surrounding air, causing the gas to sink. Gas spreading along the floor (or deck, if onboard a ship) differs from a typical fire situation with gas rising and spreading along the ceiling (where conventional point-type fire detectors are normally installed).

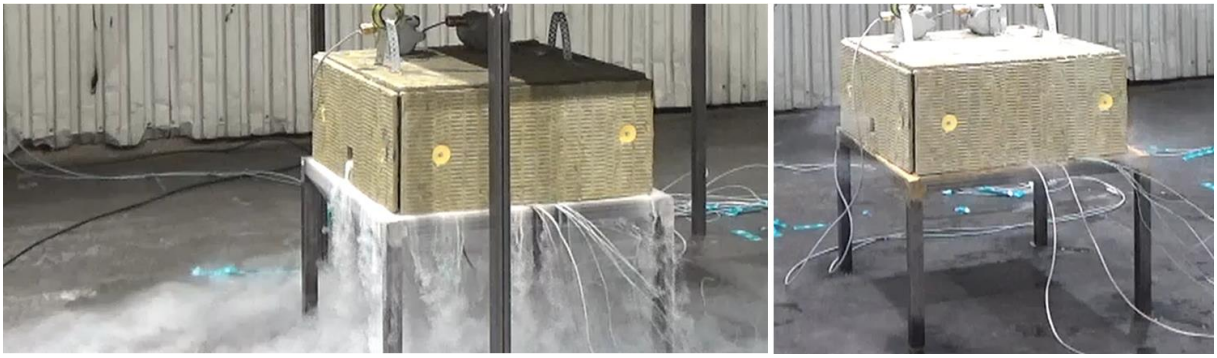

*Figure 9. Left: Sinking gases, Test 3. Right: Gas released in Test 4.*

The two smoke and heat detectors were not in operation during these tests. The CO and LEL detectors were installed inside the hood and detected the gas in Test 3, even before the time of first venting (first venting was identified by a combination of readings from the thermocouples on the battery cell and the thermal imaging; the estimated time of first venting may differ by some seconds from the actual first venting). In Test 4, the CO detector was not in operation (due to a loose contact inside the instrument) and the LEL detector detected gas shortly after first venting. This suggests that the detectors, if installed in a confined and limited space, could detect early thermal runaway.

For VA to be able to detect the smoke, the smoke first had to escape from the hood, which could be assumed to be more challenges than detecting gas/smoke in the confined space constituted by the hood. Therefore, caution should be taken if/when the results of VA are compared to the result from the smoke and heat detectors. In Test 3, VA detected the smoke 07:43 min:s after first venting. If compared with the result in Test 1 (08:39 min:s) and Test 2 (13:58 min:s), This gives an idea of detection times, under current conditions. The differences in detection times illustrate variations when it comes to detection of thermal runaway in Li-ion batteries. In Test 4, the amount of released gas/smoke was much less than that in Test 3 (cf. Figure 9), as small amounts were released over a much longer period. The individual behaviour of battery cells and the difference in the amount of released gas/smoke may be a challenge in all situations where external detection of early thermal runaway is desired.

*Table 4. Summary of detection results (min:s) from tests with a covered (hood) battery cell in a relatively open and ventilated space. F = Flame. S = Smoke. Det. = Detection.*

| Test | Video analytics | CO detector | LEL detector |
|---|---|---|---|
| 3 | 07:43 (S) | 50 ppm: -00:15<br>190 ppm: 01:43<br>>500 ppm: 07:23 | >100%: -00:15 |
| 4 | No det. | -[i] | >50%: 00:16<br>>100%: 06:11 |

[i] Not in operation during the test.

### 6.1.3 Tests 5 and 6

The results of the tests with wood-sticks on a hot plate in a ventilated room are presented in Table 5.

For the point-type detectors, a difference in time to detection was observed, namely, 16:00–17:40 min:s for Test 5 versus 04:10–06:30 min:s for Test 6. When video recordings from the two tests are compared, the amount of smoke is not significantly different, but the way the smoke rises and moves in the room is different. This, again, highlights a challenge with point-type detectors: the smoke must reach the detector(s) for detection (at an early stage). The CO detectors detected a maximum of 10 ppm CO, which was less than the lower alarm limit (50 ppm). An alarm from the heat detector was triggered in Test 6 due to the flaming combustion, for which a photo is presented in Figure 10 (right).

VA, which is not strongly sensitive to how smoke spreads, was a bit more consistent in detection times (although some spread in the result is still observable). A photo from the time of smoke detection in Test 6 is shown in Figure 10 (left).

For the detection of fires in Test 4 and Test 5 with wood sticks, the smoke and heat detectors were more suitable than the CO detector as the detection time results indicate, namely, because of the low concentrations of CO detected. This is while the detection time results are comparable for the VA and the point-type detectors, although the different locations of these detector types must be considered when comparing their results.

*Table 5. Summary of detection results (min:s) for tests with wood-sticks on an electric hot plate (ventilated space). Time is from when the hot plate was powered on.*
*F = Flame. S = Smoke. H = Heat.*

| Test | First visible smoke/flame | Video analytics | Smoke and heat detector 1 | Smoke and heat detector 2 | CO detector |
|---|---|---|---|---|---|
| 5 | 03:24 (S)<br>18:20 (F) | 08:30 (S)<br>18:27 (F) | 16:00 (S) | 16:00 (S) | 10 ppm: 17:40 |
| 6 | 02:43 (S)<br>15:00 (F) | 13:15 (S)<br>15:19 (F) | 04:30 (S) | 04:10 (S)<br>15:30 (H) | 10 ppm: 06:30 |

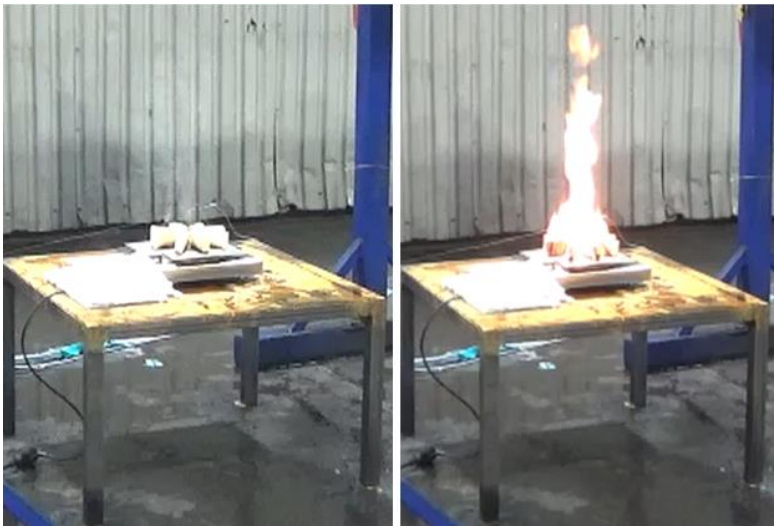

*Figure 10. Left: The fire at the time VA detected smoke in Test 6 (13:15). Right: The fire at the time the heat detector detected heat in Test 6 (15:30).*

### 6.1.4 Test 7, 8 & 9

These tests were performed with a free-standing battery cell inside a 20-ft ISO container. Detection times are presented in Table 6. Since the tests were conducted inside a container, it was not possible to determine the time to "first visible smoke" (as was presented for Test 1 and Test 2).

The detection times for the point-type detectors are in relatively good agreement when Test 7 and Test 8 are compared. However, the concentration of CO was relatively low (40 ppm as a maximum). The production of smoke in Test 9 was slow and lasted longer (as in Test 2 and Test 4), which is likely the cause for detection failure by the smoke (and heat) detectors in Test 9.

VA detected smoke in all three tests, and the detection times with VA were also shorter than those for the smoke and heat detectors (which is due to the location of the detectors). This is despite the challenging light conditions (it was relatively dark in the container). The detection time varied from 01:02 min:s to 16:56 min:s, the reason for which is not fully understood, but it is assumed to be due to the subtleties of smoke production and smoke spread which were sometimes difficult to detect against a matching background colour (white smoke against white container surfaces). When compared to the tests conducted in a room, the detection times for VA are similar, indicating that low/moderate ventilation does not have a significant impact on detection possibilities for VA.

*Table 6. Summary of detection times (min:s) for tests with a battery cell inside a 20-ft ISO container. S = Smoke. Det. = Detection.*

| Test | Video analytics | Smoke and heat detector 1 | Smoke and heat detector 2 | CO detector |
|---|---|---|---|---|
| 7 | 01:02 (S) | 12:42 | 12:40 (S) | 10 ppm: 12:02<br>40 ppm: 12:32 |
| 8 | 09:35 (S) | 10:45 | 10:15 (S) | 10 ppm: 09:30 |
| 9 | 16:56 (S) | No det. | No det. | 10 ppm: 12:11<br>30 ppm: 17:51 |

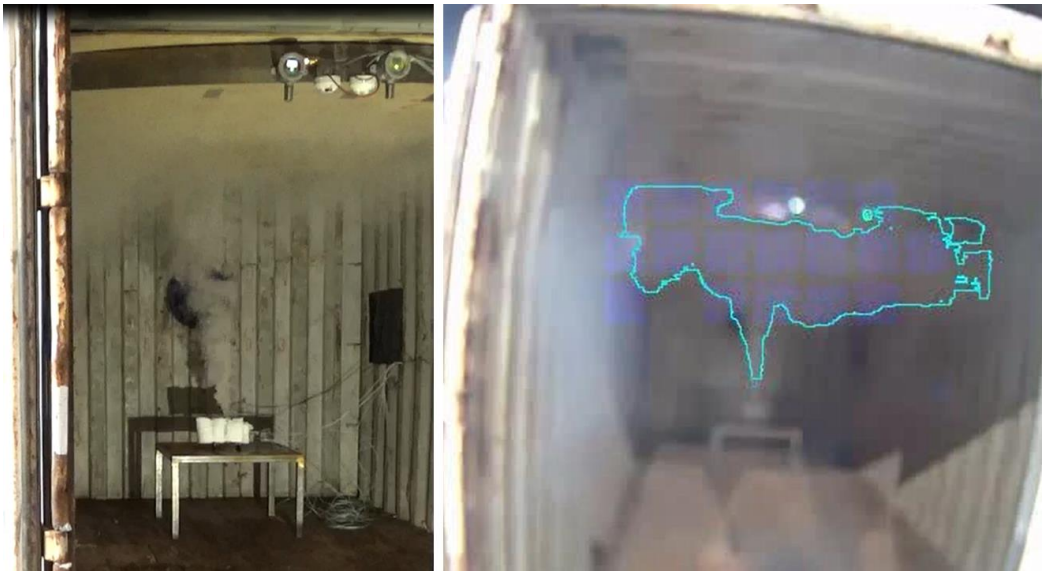

*Figure 11. Left: The battery cell during thermal runaway, smoke is rising. Right: Smoke identified by VA.*

### 6.1.5 Tests 10 and 11

Tests 10 and 11 were performed with wood-sticks on a hot plate, inside a 20-ft ISO container. Detection times are presented in Table 7. Test 10 was terminated after 22:30 min:s, when the fire was smouldering without any visible flames. The results of these tests are in line with the results of

Test 5 and Test 6 (wood-sticks in a ventilated room), which was expected (because of the same fire source/fuel). The small differences could also be ascribed to the fact that the detectors were not installed in the same positions relative to the fire source (cf. Figure 2 and Figure 6). In Test 10, the CO-concentration peaked at 130 ppm, which could be a result of the smouldering behaviour of the fire.

*Table 7. Summary of detection times (min:s) for tests with wood-sticks on an electric hot plate inside a 20-ft ISO container. Times are from when the hot plate was powered on.*
*F = Flame. S = Smoke. H = Heat.*

| Test | Video analytics | Smoke and heat detector 1 | Smoke and heat detector 2 | CO detector |
|---|---|---|---|---|
| 10 | 09:13 (S) | 15:23 | 09:20 (S) | 10 ppm: 09:40<br>50 ppm: 18:23<br>70 ppm: 19:25<br>130 ppm: 28:00 |
| 11 | 07:10 (S)<br>18:40 (F) | 09:47 | 07:44 (S) | 10 ppm: 07:55<br>20 ppm: 18:30 |

### 6.1.6 Tests 12 and 13

As in Test 3 and Test 4, the battery cells in tests 12 and 13 were covered by a hood (detection times are given in Table 8). It was again observed that the gases/smoke sank and spread along the floor (cf. Figure 12) instead of rising and spreading along the ceiling (as in the tests with a free-standing battery cell, cf. Figure 11). With the detectors installed in the same positions as in Test 7, 8, and 9 (point-type detectors in the ceiling), longer detection times were observed with the CO detector while the smoke and heat detectors failed to detect the gases. The density of CO is comparable to the density of air (1.14 kg/m$^3$ versus 1.18 kg/m$^3$ at 25°C, respectively), and if it is just somewhat hotter than the surrounding air, it could be expected to rise and reach to the CO detector. VA is not strongly sensitive to how gases spread and was able to detect the smoke.

*Table 8. Summary of detection results (min:s) from tests with a covered battery cell inside a 20-ft ISO container. Point-type detectors in the ceiling.*
*F = Flame. S = Smoke. Det. = Detection/Detector.*

| Test | Video analytics | Smoke and heat detector 1 | Smoke and heat detector 2 | CO detector |
|---|---|---|---|---|
| 12 | 10:52 (S) | No det. | No det. | 10 ppm: 15:15<br>30 ppm: 22:25 |
| 13 | 13:02 (S) | No det. | No det. | 10 ppm: 19:32 |

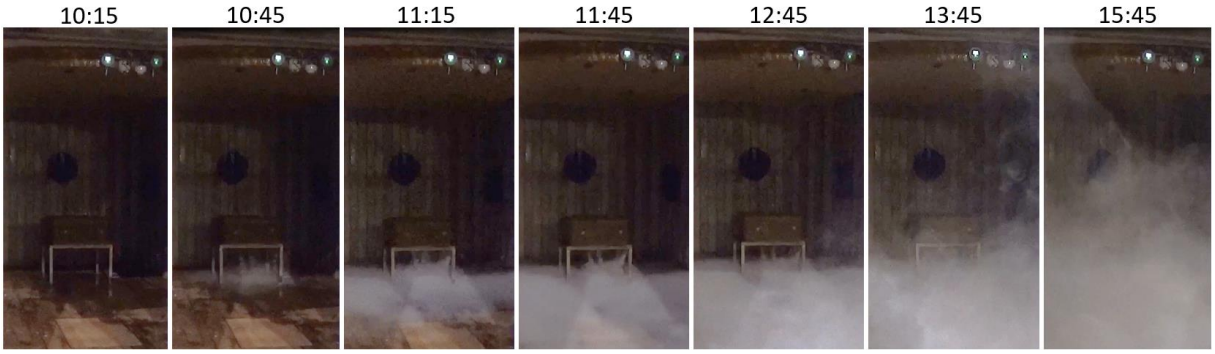


*Figure 12. Smoke from a battery cell covered by the hood (Test 12). The visible gases spread along the floor in the container. Times are related to the time of first venting (min:s) i.e., same as the detection times presented in Table 8.*

### 6.1.7 Test 14

In Test 14, the point-type detectors were inside the hood. Therefore, all three detectors were triggered shortly after, or before, the first venting. The detection before the first venting (by one of the smoke and heat detectors) may be due to the small amount of gas being released before first venting, as reported in Test 1 and Test 2. The results of VA in Test 14 are in line with those of Test 12 and Test 13.

*Table 9. Summary of detection results (min:s) for tests with a covered battery cell inside a 20-ft ISO container. Point-type detectors were inside the hood.*
*S = Smoke. H = Heat.*

| Test | Video analytics | Smoke and heat detector 1 | Smoke and heat detector 2 | CO detector |
|---|---|---|---|---|
| 14 | 09:47 (S) | -09:51 | 00:19 (S)<br>10:15 (H) | 10 ppm: 00:08<br>50 ppm: 00:15<br>>500 ppm: 08:53 |

## 6.2 Detectors without an alarm algorithm

### 6.2.1 Thermal imaging

The results of thermal imaging are presented in Table 10 (battery cells) and Table 11 (wood-sticks). All times presented are based on estimations from recordings i.e., no computer algorithm was used to interpret the data/recordings.

When the battery cell was visible to the camera lens i.e., in the tests with a free-standing battery cell, it was very easy for the thermal camera to identify the event of first venting. Examples of first venting are shown in Figure 7 and Figure 13. In Test 3, where the battery cell was covered by both a hood and an extra steel shield, it was not possible to detect any heat at all. Situations as this i.e., objects between the camera and the battery, could be expected to be relatively common e.g., in a ro-ro space. This test therefore illustrates one of the challenges with thermal imaging. In the tests with a hood covering the cell, it was possible to see the heat for some seconds. The gas/smoke sinking to the floor was, however, not possible to detect, which supports the assumption that the gas was cooled down by the hood (see explanations for Figure 9).

Thermal imaging allowed to continuously measure and record the maximum temperature in a defined area. A comparison of the maximum temperature in Test 9 (free-standing battery cell in the ISO container) and Test 12 (battery cell covered by the hood in the ISO container) is shown in Figure 14. The figure illustrates how the hood complicates the possibility to detect the temperature rise of the battery cell/hot gases.

To summarize, when the battery cell is visible to the camera lens, thermal imaging has a potential advantage over other detection technologies. In other situations, it is a technique which should be used only as a complementary means of detection, not as the sole means. As a result, a handheld thermal imaging device used by a fire patrol could be a great tool for helping with early detection.

*Table 10. Summary of the tests with battery cells.*

| Test | Source | Type of test | Thermal imaging |
|---|---|---|---|
| 1 | Battery cell | Free-standing | First venting event was clearly visible in the thermal images, and lasted for 6–8 s. The first signs of smoke visible with the naked eye before the first venting (at 03:41 min:s) were not visible in the thermal images. |
| 2 | Battery cell | Free-standing | First venting event was clearly visible in the thermal images, and lasted for 6–8 s. The first signs of smoke visible with the naked eye before the first venting (01:52 min:s) were not visible in the thermal images. |
| 3 | Battery cell | Hood + Extra shielding | Due to the shielding, it was not possible to see any heat at all. |
| 4 | Battery cell | Hood | Heat (from hot gas) was (barely) visible in the thermal images 00:20 min:s after first venting. The hot gas was barely visible (by thermal imaging), and the event lasted for approximately 1 s. Cold smoke spreading along the floor was not visible. |
| 7 | Battery cell | Free-standing | First venting event was clearly visible in the thermal images, and lasted for 6–7 s. |
| 8 | Battery cell | Free-standing | First venting event was clearly visible in the thermal images, and lasted for 6–7 s. |
| 9 | Battery cell | Free-standing | First venting event was clearly visible in the thermal images, and lasted for 6–7 s. |
| 12 | Battery cell | Hood | Heat (from hot gas) was (barely) visible in the thermal images directly after first venting. The hot gas was barely visible, and the event lasted for approximately 1–2 s. Cold smoke spreading along the floor was not visible. |
| 13 | Battery cell | Hood | Heat (from hot gas) was (barely) visible in the thermal images directly after first venting. The hot gas was barely visible, and the event lasted for approximately 1–2 s. Cold smoke spreading along the floor was not visible. |
| 14 | Battery cell | Hood | Heat (from hot gas) was (barely) visible in the thermal images directly after first venting. The hot gas was barely visible, and the event lasted for approximately 1–2 s. Cold smoke spreading along the floor was not visible. |

*Table 11. Summary of the tests with wood-sticks (min: s). The results of thermal imaging are similar to those with other detector types.*

| Test | Source | First smoke/flames visible to the naked eye | Visible in thermal imaging |
|---|---|---|---|
| 5 | Wood-sticks | 03:24 (S)<br>18:20 (F) | 09:40[i]<br>16:00[ii]<br>19:28[iii] |
| 6 | Wood-sticks | 02:43 (S)<br>15:00 (F) | 05:00[i]<br>15:00[iii] |
| 10 | Wood-sticks | The test was conducted inside the ISO container | 07:08[i]<br>09:20[iii] |
| 11 | Wood-sticks | The test was conducted inside the ISO container | 06:00[i]<br>07:00[iii] |

[i] Heat from smoke was barely visible in the thermal images.

[ii] Heat from smoke was clearly visible in the thermal images.

[iii] Heat from flames/fire visible in the thermal images.

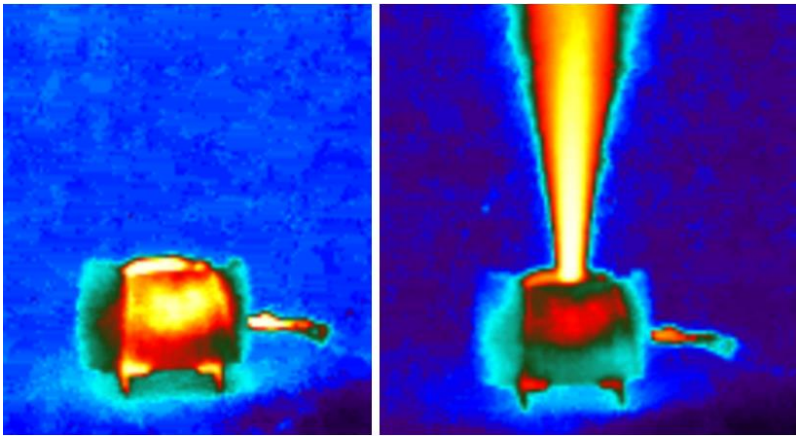

*Figure 13. The difference between the two thermal images is 0.2 s. Left: The battery cell just before first venting. Right: First venting.*

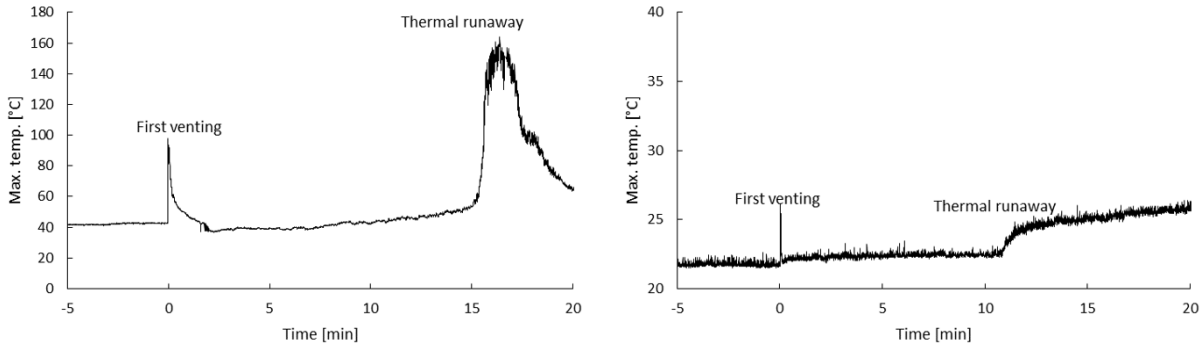


*Figure 14. With thermal imaging, it was possible to continuously measure and record the maximum temperature in a defined area. Observe the different temperature scales (Y-axes). Left: Maximum temperature in Test 9 (free standing battery cell in the ISO container). Right: Maximum temperature in Test 12 (battery cell covered by a hood, in an ISO container).*

### 6.2.2 LIDAR

The OS-2 lidar was setup to scan its environment ten times every second. The data from each scan of this time-of-flight sensor is a point cloud describing the geometry including primarily the intensity of the reflected signal. The field-of-view is limited both in the azimuth angle (the angle in the ground plane) and elevation directions. In the experiment, the sensor captures the area of interest i.e., from the floor to the ceiling.

The recordings of the point clouds were post-processed frame by frame after the experiments. Algorithms for detection and visualization were developed based on the public Open3D library. This selected approach was the simplest one possible, as the main objective was to explore the feasibility of the sensor for early detection. The idea with this detection algorithm is to give a measure of the size of changes due to the smoke/fire source in the field of view of the sensor. This assumes that no other sources of change existed in the field of view.

The tuning of this detection algorithm, with three parameters, was performed by hand to achieve an acceptable visible result. There was no attempt to define any threshold when a detection occurs. Instead, the amount of change is estimated by measurements in the point cloud. The amount is estimated as the sum of detected cubes of some arbitrary small volume. The accuracy of estimating the amount is limited by the fact that its environment is always as seen from one position; obstacles in the foreground render shadows on the background obscuring smoke in between.

To show the feasibility of detecting smoke with the lidar system, a small set of test runs have been chosen as representative. The detection algorithm has been applied frame by frame, and projection to 2D representation has been saved as a video clip. Figure 15 shows an example with a point cloud representation of the room and experimental setup for Test 1 at a time when smoke was clearly visible. The point cloud in the figure shows the same experiment setup as the photo in Figure 8. Figure 16 is based on the same test i.e., Test 1. The amount of smoke is plotted over time and corresponds to the volume of the red cubes in Figure 15. The figure clearly shows the history of a first venting event followed by a pause before the amount of smoke rapidly increases to a peak, then decreased, and thereafter slowly fades away.

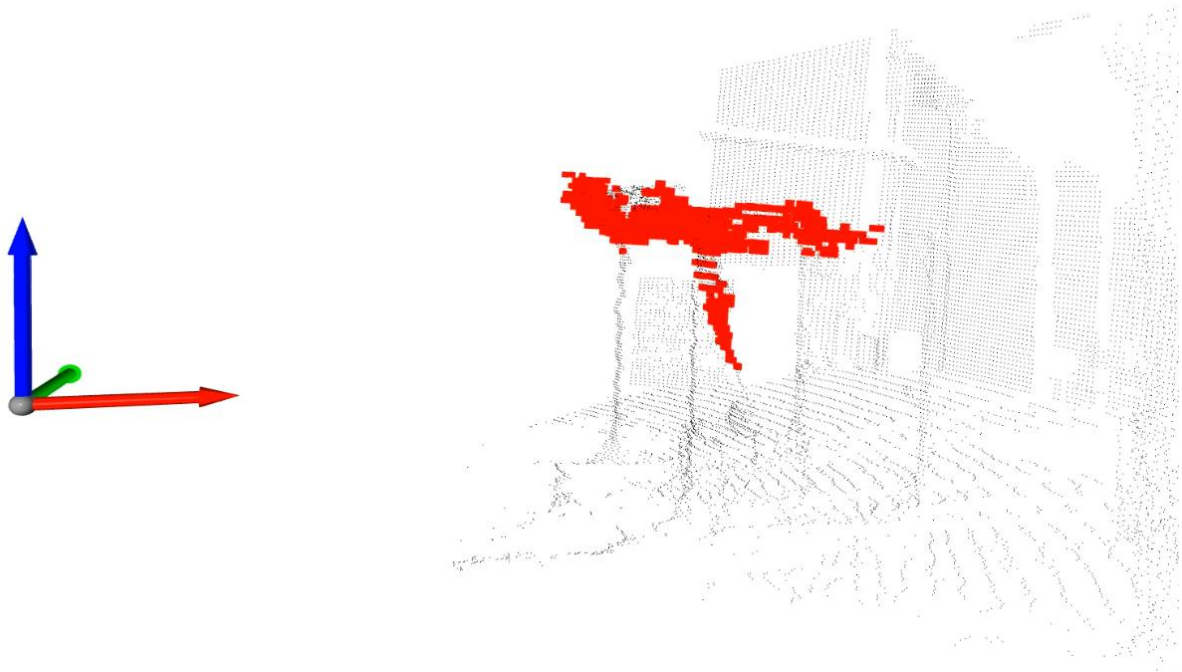

*Figure 15 Extract from Test 1 in 3D displaying the room and the detected smoke. The red-green-blue coordinate frame, with arrows of one meter length, shows the location of the sensor. The rising smoke is depicted as a set of red dots or cubes in the dark point cloud representing the room.*

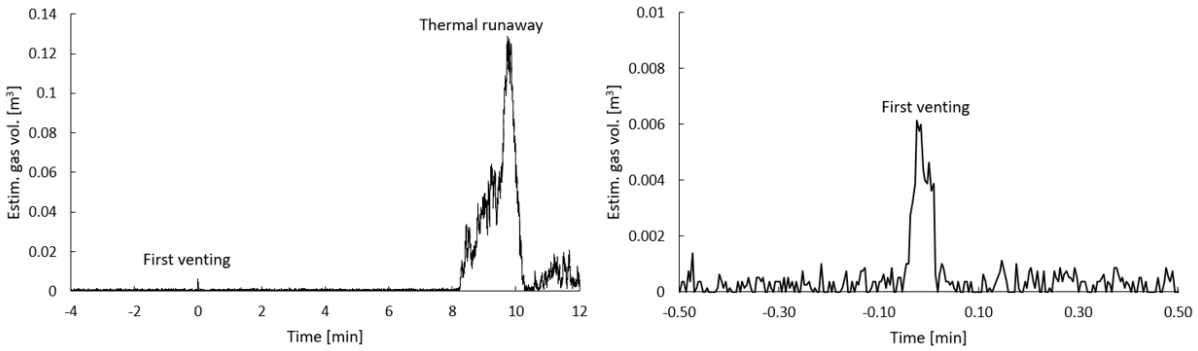


*Figure 16 History of detected smoke from Test 1 in terms of the smoke volume (y-axis) versus time (x-axis). The figure to the right illustrates a magnification around the first 0.5 min of the test, showing the first venting event more clearly. After a pause of 500 seconds (08:20 min:s), the smoke generation restarts in the form of a thermal runaway event (left figure).*

Figure 17 shows a sequence of snap shots from Test 12 taken from the same moments in time as in Figure 12 such that it is possible to get a visual correspondence. The smoke spreads on the floor of the container. As the smoke approaches the opening of the container close to the sensor, the sensor can no longer see the extent of all smoke since the smoke near the sensor obscures what is behind it. Nevertheless, it can be concluded that smoke on the floor is quite possible to detect. The shape of the detected smoke would be different if a design choice was to place the sensor elsewhere.

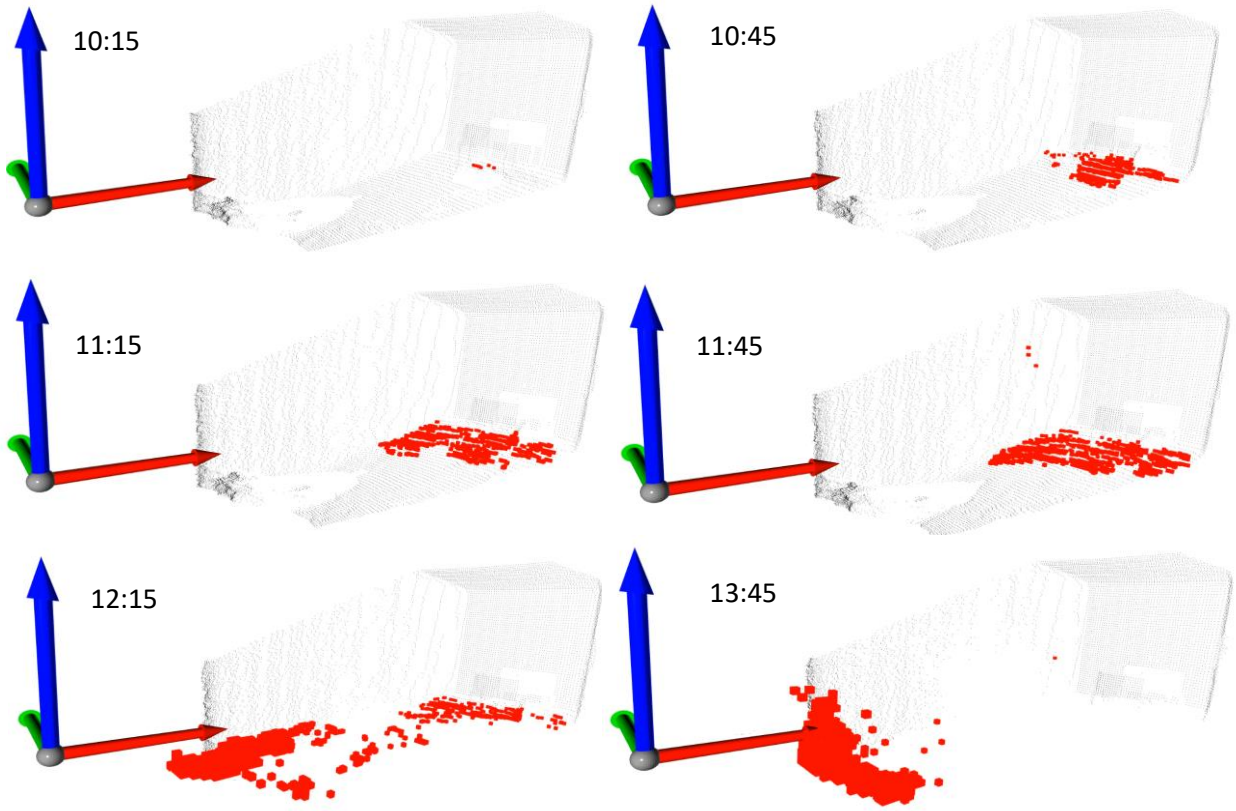


*Figure 17 Smoke spreads on the floor of the container in Test 12. The smoke is case depicted as small red cubes. The sequence of frames corresponds with same moments in time as in Figure 12. The coordinate frame shows the location of the lidar.*

It can be concluded that the lidar can detect the generated smoke, although this is dependent both on the size distribution and on the number concentration of the aerosols (dry or wet). The sensor cannot detect the heat or gas.

The detection algorithm has room for improvements. For instance, the revision mechanism of this sensor lacked one feature that would have been useful, namely, it was restricted to only one return hit per transmitted pulse. As the smoke can be described as a sparse object, some points will continue through and others will bounce, and this could be used to improve detection. The detection is also improved in case there is a static background in the range of the sensor revealing an object blocking the rays. Further, an obvious challenge for the method used above is how to handle legitimate changes in the scene that do not have any relation to the smoke generation. With more data, it would be possible to detect smoke by an approach based on machine learning. The sensor is rather expensive, but in a real installation it could typically be used for multiple purposes to motivate its cost.

# 7 Discussion

The study was aimed at the evaluation of potential detection principles and challenges for early detection of thermal runaway in batteries. Following the assumption that thermal runaway starts in a single cell, the tests were done at cell level. The results relate to cells e.g., the first venting may not be possible to observe outside of a battery or battery pack; the tests were run on cell level as a first observation of events and "screening" of technologies. Typically, a very small amount of smoke could be observed 2–4 min before the first venting. First venting was typically observed 10–15 min before thermal runaway. Future research should address when action must be taken to prevent propagation to other cells, as this was not part of the current study.

When the point-type detectors were installed inside the hood, they were able to detect gas/smoke at the time of, or shortly before, the first venting. In this test, the heat detector triggered an alarm after 10:15 min:s. When the battery cell was free-standing inside the ISO container, the point-type detectors were able to detect gas/smoke 5–15 min after the first venting, a typical detection time was around 10 min. In the tests with a free-standing battery cell in a ventilated room, the point-type detectors all failed to the detect any gas or smoke (or heat).

When the battery cell was covered by a hood, the (visible) gas/smoke was cooled down (supported by thermal imaging) before exiting the hood. This resulted in gas/smoke spreading along the floor instead of rising and spreading along the ceiling. The opening on the hood compartment (50 mm × 50 mm) was placed at lower heights. This probably resulted in longer residence time of the gas inside the hood and thus enhanced cooling. Had the opening been at higher heights (which is an equally likely leak scenario), the gas would have been able to escape faster with less cooling.

As a direct consequence of the sinking gas, the smoke and heat detectors installed above the battery cell were not able to detect the smoke. The CO sensor, also installed above the battery cell, was able to detect 10–30 ppm of CO when the battery cell was covered by the hood. The density of CO is close to that of air and could explain why CO moved upward and spread in the container. There might also be other gas species e.g., hydrogen, that can rise in this situation. This was not covered by the current study but should be included in further research. Gas/smoke spreading along the floor, instead of rising, could be a challenge in real scenarios; detectors are normally installed on the ceiling.

When the point-type detectors were installed inside the hood, there was no obvious difference between smoke, CO, and LEL detectors. A reason could be the relatively large amount of gas/smoke produced, compared to the limited volume of the hood.

To summarize the results from the tests with point-type detectors, they were all able to detect the gas/smoke from the battery cell in these tests. However, *the gas/smoke must reach the detector*, which could be a challenge in larger, open and ventilated spaces. If the gas/smoke is cooled down (e.g., by car chassis or a ship's steel structure), it may sink and spread along the floor (or deck, if on board a ship).

Video analytics, thermal imaging, and LIDAR are not limited to a single detection point, as they monitor the three-dimensional space. This is beneficial since gas/smoke or heat does not need to reach the location of such detectors for detection. VA was able to detect smoke in all of the tests, except Test 4. However, the amount of smoke from the first venting was not sufficient for detection (with the current device settings). Typically, VA detected smoke 10 min after the first venting i.e., during the thermal runaway of the battery cell. Thermal imaging was able to detect the hot gas released during the first venting – as long as the hot gas was visible to the camera lens. The LIDAR

was able to detect smoke and can also estimate the amount of smoke detectable from its location. One benefit with thermal imaging and LIDAR is that they are much less sensitive (LIDAR is much less sensitive, than for example a camera, sun reflections typically do not blind the lidar, and it works in bright as well as dark conditions) to the light conditions compared to VA.

In the current study, 50 % SOC was used in all the tests. This SOC was selected to avoid ignition of the gases, but also to be representative of the SOC in a conventional BEV. The SOC, as well as the heating procedure to trigger thermal runaway may affect the composition of the gas(es) released [7]. This in turn could have an impact on the detection, although this was not covered in this study.

## 7.1 Proposed further research

The results of this study indicate that further research is needed to address early detection of thermal runaway. Specifically, the following is proposed:

- The smoke/visible gas was cooled down, so it sank and spread along the floor. CO, however, reached the CO detector in the ceiling. This indicates that some of the gaseous species (e.g., CO, and probably hydrogen, although not addressed in this study) can move upward. Further research should conduct full-scale tests with BEVs to better understand how their gas/smoke spread can be detected under different conditions. Such work should also address the risk of gas accumulation and a subsequent ignition.
- As optical gas imaging (OGI) [8, 9] is based on a camera technique (and is able to monitor the three-dimensional space), it has the same advantage as the VA but with a possibility of being more sensitive and specific. It was not possible to include OGI in the current study, but it should be evaluated in further research.
- The impact of SOC and type of cell, with regard to buoyancy of smoke and self-ignition should be further addressed.
- Early external detection of thermal runaway is associated with challenges. It is proposed to further explore if communication with the battery management system (BMS) could be a suitable and better means to detect thermal runaway in its early stages.
- Further research should address potential actions to be taken in relation to the time of detection/first venting/thermal runaway i.e., what can be done at what time?
- Finally, tests should be performed with a battery pack, as the next step to tests with single cells. This can help further examine the conclusions presented in the current study and to gain knowledge on larger and more intricate systems.

# 8 Conclusion

Main author of the chapter: Sixten Dahlbom, RISE

Based on the study results, it can be concluded that early detection of thermal runaway in batteries is possible in principle. However, detection is a matter of circumstances e.g., ventilation, gas/smoke production and the location of the detector(s). The results indicate that detection in a small and confined place is relatively manageable, but detection in a large and open space could be a bigger challenge. If the gas/smoke is cooled down sufficiently, it sinks and spreads along the floor/deck, instead of rising and spreading along the ceiling/deckhead. This would be a challenge with current smoke detectors installed on the ceiling. Shielding may be a problem, especially with LIDAR and thermal imaging. Future research should address full-scale tests and it is recommended to examine OGI as another means of detection.

# 9 References


1. Griffis, T.E. *Ro/ro vessel capacity to remain tight with EV, heavy equipment growth: Wallenius CEO*. 2023 [cited 2023 September 27]; Available from: https://www.joc.com/article/roro-vessel-capacity-remain-tight-ev-heavy-equipment-growth-wallenius-ceo_20230613.html.
2. Zeinali, D., Stølen R., and R. Synnøve Skilbred, *D09.2 – Developed ro-ro spaces fire detection solutions and recommendations*. 2023, FRN. p. 129.
3. Andersson S., Olsson K., and Willstrand O., *IR09.14 – Early Detection of Thermal Runaway in Lithium-ion Batteries*. 2023, RISE. p. 21.
4. *DNV has published the July 2023 edition of the rules for classification of ships*. 2023 [cited 2023 September 27]; Available from: https://www.dnv.com/news/dnv-has-published-the-july-2023-edition-of-the-rules-for-classification-of-ships-245133.
5. International Organization for Standardization (ISO), *Series 1 freight containers – Classification, dimensions and ratings (ISO 668:2020, IDT)*. 2020.
6. Comité Européen de Normalisation (CEN), *Fire detection and fire alarm systems – Part 7: Smoke detectors – Point smoke detectors that operate using scattered light, transmitted light or ionization (EN 54-7:2018)*. 2018.
7. Willstrand, O., et al., *Impact of different Li-ion cell test conditions on thermal runaway characteristics and gas release measurements.* Journal of Energy Storage, 2023. **68**: p. 107785.
8. *Optical Gas Imaging*. 2023 [cited 2023 September 27]; Available from: https://www.flir.com/instruments/optical-gas-imaging/.
9. *How does it work?* [cited 2023 September 27]; Available from: https://www.tunable.com/technology.

# 10 Indexes

## 10.1 Index of tables



## 10.2 Index of figures